



# Magnetic order and crystal structure study of YNi<sub>4</sub>Si-type NdNi<sub>4</sub>Si



Jinlei Yao<sup>a</sup>, O. Isnard<sup>b,c</sup>, A.V. Morozkin<sup>d,\*</sup>, T.I. Ivanova<sup>e</sup>, Yu.S. Koshkid'ko<sup>f,g</sup>, A.E. Bogdanov<sup>e</sup>, S.A. Nikitin<sup>e</sup>, W. Suski<sup>f,h</sup>

<sup>a</sup> Research Center for Solid State Physics and Materials, School of Mathematics and Physics, Suzhou University of Science and Technology, Suzhou 215009, China

<sup>b</sup> Université Grenoble Alpes, Inst NEEL, BP166, Grenoble F-38042, France

<sup>c</sup> CNRS, Institut NEEL, 25 rue des martyrs, Grenoble F-38042, France

<sup>d</sup> Department of Chemistry, Moscow State University, Leninskie Gory, House 1, Building 3, GSP-2, Moscow 119992, Russia

<sup>e</sup> Physics Department, Moscow State University, Moscow 119992, Russia

<sup>f</sup> International Laboratory of High Magnetic Fields and Low Temperatures, Wrocław, Poland

<sup>g</sup> VSB-Technical University of Ostrava, Ostrava-Poruba 70833, Czech Republic

<sup>h</sup> Polish Academy of Sciences, Trzebiatowski Institute of Low Temperatures and Structure Research, P.O. Box 1410, 50-950 Wrocław 2, Poland

## ARTICLE INFO

### Article history:

Received 3 October 2014

Received in revised form

11 November 2014

Accepted 16 November 2014

Available online 24 November 2014

### Keywords:

Rare-earth compounds

Magnetic properties

Magnetocaloric effect

Neutron diffraction

Magnetic structure

## ABSTRACT

Magnetic measurements and neutron powder diffraction investigation of the magnetic structure of the orthorhombic YNi<sub>4</sub>Si-type (space group *Cmmm*) NdNi<sub>4</sub>Si compound are presented. The magnetocaloric effect of NdNi<sub>4</sub>Si is calculated in terms of the isothermal magnetic entropy change and it reaches the maximum value of  $-3.3$  J/kg K for a field change of 50 kOe near  $T_C = 12$  K. Below  $\sim 12$  K, NdNi<sub>4</sub>Si exhibits a commensurate *b*-axis collinear ferromagnetic ordering with the *Cmm'm* magnetic space group in a zero magnetic field. At 1.5 K, the neodymium atoms have the magnetic moment of  $2.37(5) \mu_B$ . The orthorhombic crystal structure and its thermal evolution are discussed in comparison with the CaCu<sub>5</sub>-type compound.

© 2014 Elsevier Inc. All rights reserved.

## 1. Introduction

Recently, the orthorhombic derivative of the CaCu<sub>5</sub>-type, namely the YNi<sub>4</sub>Si-type (space group *Cmmm*), RNi<sub>4</sub>Si compounds ( $R = Y, La, Ce, Sm, Gd-Ho$ ) were reported [1]. These compounds supplement the known series of the CaCu<sub>5</sub>-type RNi<sub>5</sub> compounds and RNi<sub>4</sub>Si solid solutions [2,3]. The orthorhombic distortion of parent CaCu<sub>5</sub>-type compounds may be considered a prospective route for optimizing their magnetic and hydrogen storage properties [4–6]. In order to test its feasibility, it requires a systematic investigation of the magnetic properties of YNi<sub>4</sub>Si-type RNi<sub>4</sub>Si, which can be in comparison with those of the well-known CaCu<sub>5</sub>-type RNi<sub>5</sub> and RNi<sub>4</sub>Si compounds.

The early reports of the magnetic properties and structures of CaCu<sub>5</sub>-type RNi<sub>5</sub> and RNi<sub>4</sub>Si [7–11] and YNi<sub>4</sub>Si-type RNi<sub>4</sub>Si [1,12,13] ( $R = Gd, Tb, Dy$ ) permit us to draw the following preliminary conclusions. In the case of {Tb, Dy}Ni<sub>4</sub>Si the ferromagnetic ordering temperature increases from the CaCu<sub>5</sub>-type RNi<sub>5</sub> across CaCu<sub>5</sub>-type RNi<sub>4</sub>Si to YNi<sub>4</sub>Si-type RNi<sub>4</sub>Si, whereas the Curie point decreases from GdNi<sub>5</sub> to the CaCu<sub>5</sub>-type GdNi<sub>4</sub>Si and the Curie temperatures of

CaCu<sub>5</sub>-type and YNi<sub>4</sub>Si-type GdNi<sub>4</sub>Si are the same. We suggest that the transformation of their magnetic properties in the orthorhombic distortion of CaCu<sub>5</sub>-type lattice results from the initial *ab*-plane ferromagnetic-like ordering of Tb and Dy sublattices and possible *c*-collinear ferromagnetic ordering of Gd sublattice. The Ni ions have little to no magnetic moments in these compounds.

The initial CaCu<sub>5</sub>-type NdNi<sub>5</sub> shows ferromagnetic ordering below 7.2 K with isothermal magnetic entropy change of  $-8.45$  J/kg K for a field change of 0–50 kOe [14,15]. The substitution of Si for Ni in the NdNi<sub>4</sub>Si solid solution leads to increase of Curie point from 7.2 to 9.2 K and decrease of isothermal magnetic entropy change from  $-8.45$  J/kg K to  $-7.3$  J/kg K for a field change of 0–50 kOe [16].

This work aims to understand the effects of orthorhombic distortion from the parent CaCu<sub>5</sub>-type NdNi<sub>5</sub> to the YNi<sub>4</sub>Si-type NdNi<sub>4</sub>Si compound through the magnetic measurements and neutron powder diffraction.

## 2. Material and methods

The NdNi<sub>4</sub>Si sample was prepared by arc melting of the stoichiometric amounts of Nd (99.9 wt%), Ni (99.95 wt%) and Si (99.99 wt%). The sample was annealed at 1070 K for 200 h in an

\* Corresponding author.

E-mail address: [morozkin@tech.chem.msu.ru](mailto:morozkin@tech.chem.msu.ru) (A.V. Morozkin).

argon-filled and sealed quartz tube and subsequently quenched in ice-cold water. The structure, purity and composition of the polycrystalline sample were evaluated using powder X-ray diffraction (XRD) and electron microprobe analysis. The XRD data were obtained on a Rigaku D/MAX-2500 diffractometer (CuK $\alpha$ 1 radiation,  $2\theta=10\text{--}80^\circ$ , step  $0.02^\circ$ , 1 s/step). An INCA-Energy-350 X-ray EDS spectrometer (Oxford Instruments) on A Jeol JSM-6480LV scanning electron microscope (20 kV accelerating voltage, beam current 0.7 nA and beam diameter  $50\ \mu\text{m}$ ) was employed to perform the microprobe analyses of the sample. Signals from three points were averaged and estimated standard deviations were 1 at% for Nd (measured by L-series lines), 1 at% for Ni and 1 at% for Si (measured by K-series lines).

DC magnetization of the polycrystalline NdNi $_4$ Si sample was measured on a commercial Physical Property Measurement System (Quantum Design PPMS-DynaCool) in the temperatures range of 5–300 K with an applied magnetic field of 5 kOe in the zero-field-cooled (ZFC) and field-cooled (FC) modes. The isothermal saturation magnetization was measured for the magnetic field change from 0 to 50 kOe at various temperatures.

Neutron diffraction experiments were carried out at the high flux reactor of the Institut Laue Langevin (Grenoble, France). The data were collected in a zero magnetic field on the two-axis D1B powder diffractometer equipped with a 1300 cell curved detector spanning the  $2\theta$  range of  $130^\circ$  [17]. The temperature ranges were 128–30 K with a step of  $\sim 10$  K and 25–1.5 K with a step of  $\sim 5$  K. The neutron wavelength of 2.5238 Å was selected by the (002) reflection of a pyrolytic graphite monochromator and the  $2\theta$  step was  $0.1^\circ$ .

### 3. Theory/calculation

The unit cell data were derived from the powder XRD using the Rietan program [18,19] in the isotropic approximation at room temperature. The paramagnetic susceptibility was fitted to the Curie–Weiss law to obtain the effective magnetic moment and paramagnetic Curie temperature [20]. Magnetocaloric effect (MCE) was calculated in terms of the isothermal magnetic entropy change,  $\Delta S_m$ , using the magnetization vs. field data obtained near the magnetic transition and employing the thermodynamic Maxwell equations [21]. The neutron diffraction data were refined with the FULLPROF program [22]. The magnetic space groups [23,24] were used for the analysis of neutron diffraction data.

## 4. Results

### 4.1. Crystal structure

Both the microprobe and X-ray powder analyses show that NdNi $_4$ Si is a single-phase sample. The microprobe analysis yielded the Nd $_{17(1)}$ Ni $_{68(1)}$ Si $_{15(1)}$  composition, and the X-ray powder analysis

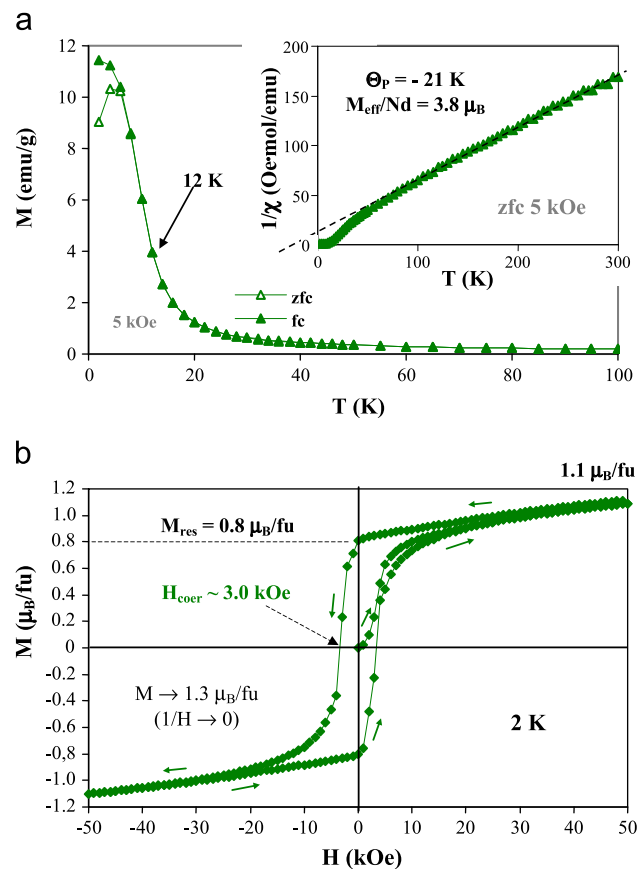


**Fig. 1.** (a) Magnetization and inverse magnetic susceptibility of NdNi $_4$ Si as a function of temperature in 5 kOe and (b) magnetization vs. magnetic field of NdNi $_4$ Si at 2 K.

**Table 1**  
Atomic positions for the 2a, 4i and 4f sites of the  $Cmmm^a$  space group (retained by NdNi $_4$ Si) with the corresponding symmetry operators and magnetic space group  $Cmm'm^b$  (retained by  $b$ -axis collinear ferromagnetic ordering of NdNi $_4$ Si) with corresponding magnetic symmetry operators.

Site	Atom	$x/a$	$y/b$	$z/c$	Symmetry operator	Magnetic symmetry operator
2a	Tb $^1$	0	0	0	$Pmmm^c$	$Pmm'm^f$
	Tb $^2$	1/2	1/2	1/2	$Pmmm/[1/2\ 0\ 1/2]$	$Pmm'm \times [1/[1/2\ 0\ 1/2]]$
4i	Ni1 $^1$	0	$y$	0	$Pm2m^d$	$Pm2m^g$
	Ni1 $^2$	0	$-y$	0	$\{2_x, \mathbf{m}_y, 2_z, \bar{1}\}$	$1' \times \{2_x, \mathbf{m}_y, 2_z, \bar{1}\}$
	Ni1 $^3$	1/2	$1/2+y$	0	$Pm2m/[1/2\ 1/2\ 0]$	$Pm2m \times [1/[1/2\ 1/2\ 0]]$
	Ni1 $^4$	1/2	$1/2-y$	0	$\{2_x, \mathbf{m}_y, 2_z, \bar{1}\}/[1/2\ 1/2\ 0]$	$1' \times \{2_x, \mathbf{m}_y, 2_z, \bar{1}\}/[1/2\ 1/2\ 0]$
4f	Ni2 $^1$	1/4	1/4	1/2	$P2_1/n^e$	$P2_1'n^h$
	Ni2 $^2$	$-1/4$	1/4	1/2	$\{\mathbf{m}_x, 2_x/[1/2\ 1/2\ 0], 2_y, \mathbf{m}_y/[1/2\ 1/2\ 0]\}$	$\{\mathbf{m}_x, 1' \times 2_x/[1/2\ 1/2\ 0], 2_y, 1' \times \mathbf{m}_y/[1/2\ 1/2\ 0]\}$
	Ni2 $^3$	1/4	$-1/4$	1/2	$\{\mathbf{m}_x/[1/2\ 1/2\ 0], 2_x, 2_y/[1/2\ 1/2\ 0], \mathbf{m}_y\}$	$\{\mathbf{m}_x/[1/2\ 1/2\ 0], 1' \times 2_x, 2_y/[1/2\ 1/2\ 0], 1' \times \mathbf{m}_y\}$
	Ni2 $^4$	$-1/4$	$-1/4$	1/2	$P2_1/n/[1/2\ 1/2\ 0]$	$P2_1'n/[1/2\ 1/2\ 0]$

<sup>a</sup>  $Cmmm = \{1, \mathbf{m}_x, \mathbf{m}_y, \mathbf{m}_z, \bar{1}, 2_x, 2_y, 2_z\} \times \{1, [1/2\ 1/2\ 0]\} = Pmmm \times \{1, [1/2\ 1/2\ 0]\}$ .

<sup>b</sup>  $Cmm'm = \{1, \mathbf{m}_x, 1' \times \mathbf{m}_y, \mathbf{m}_z, 1' \times \bar{1}, 1' \times 2_x, 2_y, 1' \times 2_z\} \times \{1, [1/2\ 1/2\ 0]\} = \{1, \mathbf{m}_x, 2_y, \mathbf{m}_z\} \times \{1, 1' \times \bar{1}\} \times \{1, [1/2\ 1/2\ 0]\} = Pmm'm \times \{1, [1/2\ 1/2\ 0]\}$ .

<sup>c</sup>  $Pmmm = \{1, \mathbf{m}_x, \mathbf{m}_y, \mathbf{m}_z, \bar{1}, 2_x, 2_y, 2_z\}$ .

<sup>d</sup>  $Pm2m = \{1, \mathbf{m}_x, 2_y, \mathbf{m}_z\}$ .

<sup>e</sup>  $P2_1/n = \{1, \mathbf{m}_z, 2_x/[1/2\ 1/2\ 0], \bar{1}/[1/2\ 1/2\ 0]\}$ .

<sup>f</sup>  $Pmm'm = \{1, \mathbf{m}_x, 1' \times \mathbf{m}_y, \mathbf{m}_z, 1' \times \bar{1}, 1' \times 2_x, 2_y, 1' \times 2_z\} = Pm2m \times \{1, 1' \times \mathbf{m}_y\}$ .

<sup>g</sup>  $Pm2m = Pm2m = \{1, \mathbf{m}_x, 2_y, \mathbf{m}_z\}$ .

<sup>h</sup>  $P2_1'n = \{1, \mathbf{m}_z, 1' \times 2_x/[1/2\ 1/2\ 0], 1' \times \bar{1}/[1/2\ 1/2\ 0]\} = \{1, \mathbf{m}_z\} \times \{1, 1' \times 2_x/[1/2\ 1/2\ 0]\}$ .

confirmed the  $\text{YNi}_4\text{Si}$ -type structure with the  $Cmmm$  space group. The lattice parameters were refined as  $a=0.51354(2)$  nm,  $b=0.83006(3)$  nm,  $c=0.39707(2)$  nm,  $V=0.16926(4)$  nm<sup>3</sup>,  $b/(3^{1/2}a)=0.93320(3)$ , and the atomic sites Nd ( $2a$ ) [0, 0, 0], Ni1 ( $4i$ ) [0, 0.3424(5), 0], Ni2 ( $4f$ ) [1/4, 1/4, 1/2] and Si ( $2c$ ) [0, 1/2, 1/2] ( $R_F=4.5\%$ ). The atomic positions for the Nd  $2a$ , Ni1  $4i$  and Ni2  $4f$  sites in the  $Cmmm$  space group with the corresponding symmetry operators are given in Table 1.

#### 4.2. Magnetic properties and magnetocaloric effect

The zero-field-cooled (ZFC) and field-cooled (FC) magnetization data recorded during heating in 5 kOe are shown in Fig. 1a. The FC data are indicative of a typical ferromagnet, while the ZFC data suggest presence of weak competing antiferromagnetic interactions, which can be easily overcome in small magnetic fields. The paramagnetic susceptibility of  $\text{NdNi}_4\text{Si}$  follows the Curie–Weiss law in the temperature range 90–300 K (inset in Fig. 1a). The fit to the Curie–Weiss law yielded a paramagnetic Weiss temperatures  $\theta_p=-21(5)$  K and the effective moment per formula unit  $M_{\text{eff}}=3.8 \mu_B/\text{f.u.}$  The negative  $\theta_p$  can be seen as the development of antiferromagnetic-type interactions, which is also observed in the ferromagnetic  $\text{SmNi}_4\text{Si}$  compound [25]. The refined  $M_{\text{eff}}$  is close to the theoretical magnetic moment of  $\text{Nd}^{3+}$  ( $3.62 \mu_B$ ) [26], indicating Nd is trivalent in the compound. However the neutron diffraction studies do not confirm the presence of magnetic moments on Ni, and thus only Nd atoms are assumed to carry localized magnetic moments. In this case, the effective magnetic moment of the Nd atoms is  $3.8 \mu_B$ , and a slight increase of  $\sim 0.2 \mu_B$  over the theoretical value can be attributed to the polarization of conduction electrons, predominantly the Nd  $5d$  ones, through the  $4f$ – $5d$  exchange interactions.

The magnetization vs. magnetic field for  $\text{NdNi}_4\text{Si}$  at 2 K is plotted in Fig. 1b. A rapid increase in the magnetization at low fields is typical for a ferromagnet and is attributed to the domain growth. However, a subsequent slow linear increase and non-saturating behavior is indicative of the competing antiferromagnetic interactions and/or strong anisotropy. A strong magnetic anisotropy is likely to be present in the  $\text{NdNi}_4\text{Si}$  structure and does not allow the magnetic moments to be fully oriented in the magnetic field. The saturation magnetic moment reaches the value of  $1.1 \mu_B/\text{Nd}$  in 50 kOe, which is significantly smaller than the theoretical saturation moment  $3.27 \mu_B$  of  $\text{Nd}^{3+}$  [26].  $\text{NdNi}_4\text{Si}$  shows the hysteresis at 2 K with residual magnetization  $M_{\text{res}}=0.8 \mu_B/\text{f.u.}$  and coercive field  $H_{\text{coer}}=3.4$  kOe (Fig. 1b). Existence of significant coercivity in the hysteresis cycle may be an indication of the presence of uniaxial magnetic anisotropy in the  $\text{NdNi}_4\text{Si}$  compound, which is verified as a ferromagnetic ordering along the  $b$  axis through the neutron diffraction studies below.

The magnetocaloric effect of  $\text{NdNi}_4\text{Si}$  in terms of the isothermal magnetic entropy change,  $\Delta S_m$ , was calculated from the saturation magnetization data (Fig. 2a). A numerical integration is performed using the following formula:  $\Delta S(T)_{\text{mag}} = \sum M_{i+1} - M_i/T_{i+1} - T_i \Delta H$ , where  $\Delta H$  is a magnetic field step and  $M_i$  and  $M_{i+1}$  are the values of magnetization at temperatures  $T_i$  and  $T_{i+1}$ , respectively [21]. The magnetic entropy change,  $\Delta S_m$ , for  $\Delta H=0-50$  kOe is plotted in Fig. 2b. As expected for a second order magnetic transition,  $\Delta S_m$  peaks around the Curie temperature and has a maximum value of  $-3.3$  J/kg K.

#### 4.3. Magnetic structure

Above 10 K, the neutron diffraction patterns of  $\text{NdNi}_4\text{Si}$  in a zero applied field correspond to the paramagnetic state, and at  $T_C^{\text{ND}} \sim 10$  K a set of commensurate magnetic reflections with a  $\mathbf{K}_0=[0, 0, 0]$  wave vector indicates the magnetic ordering of  $\text{NdNi}_4\text{Si}$  (Fig. 3). The

ordering temperature found from the neutron diffraction study is in good agreement with the value deduced from the magnetization measurements of  $T_C \sim 12$  K (Figs. 1a and 4a).

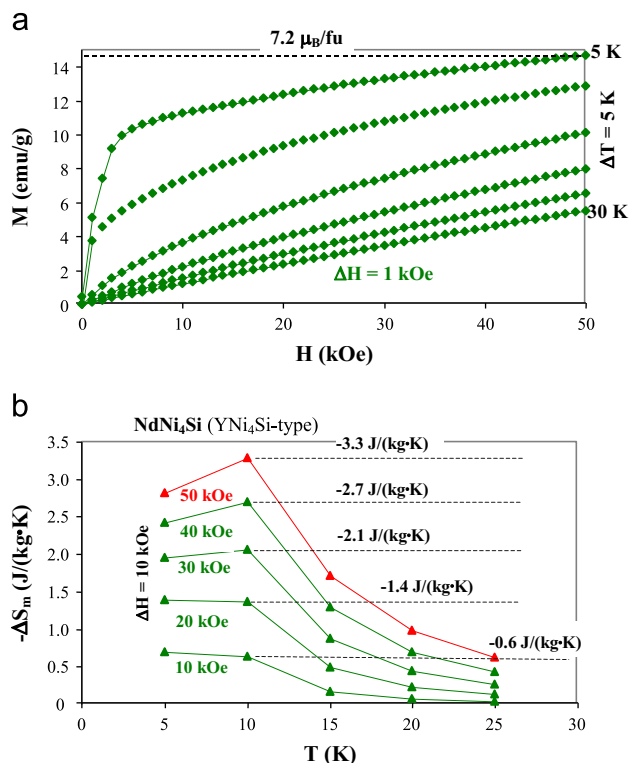


Fig. 2. (a) Magnetization vs. magnetic field and (b) the isothermal entropy change,  $-\Delta S_m$ , of  $\text{NdNi}_4\text{Si}$  around the magnetic transition.

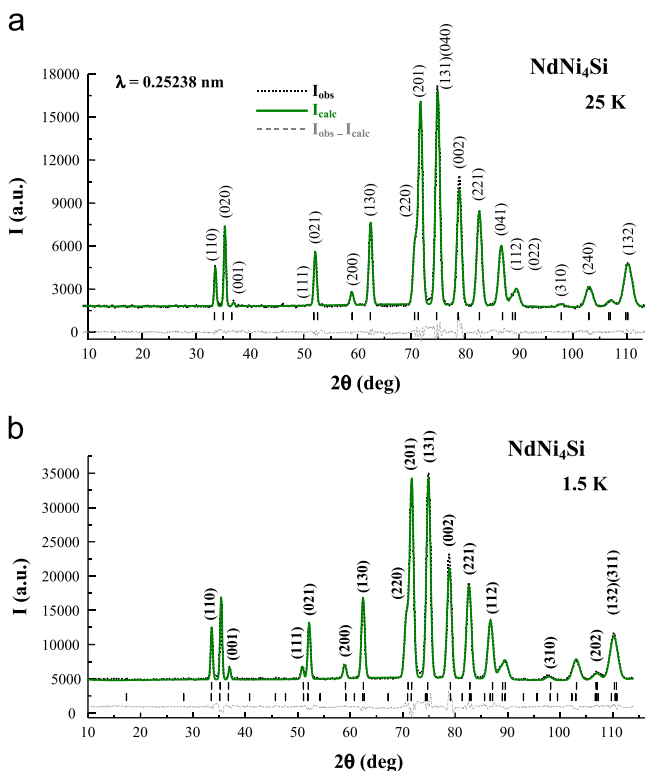
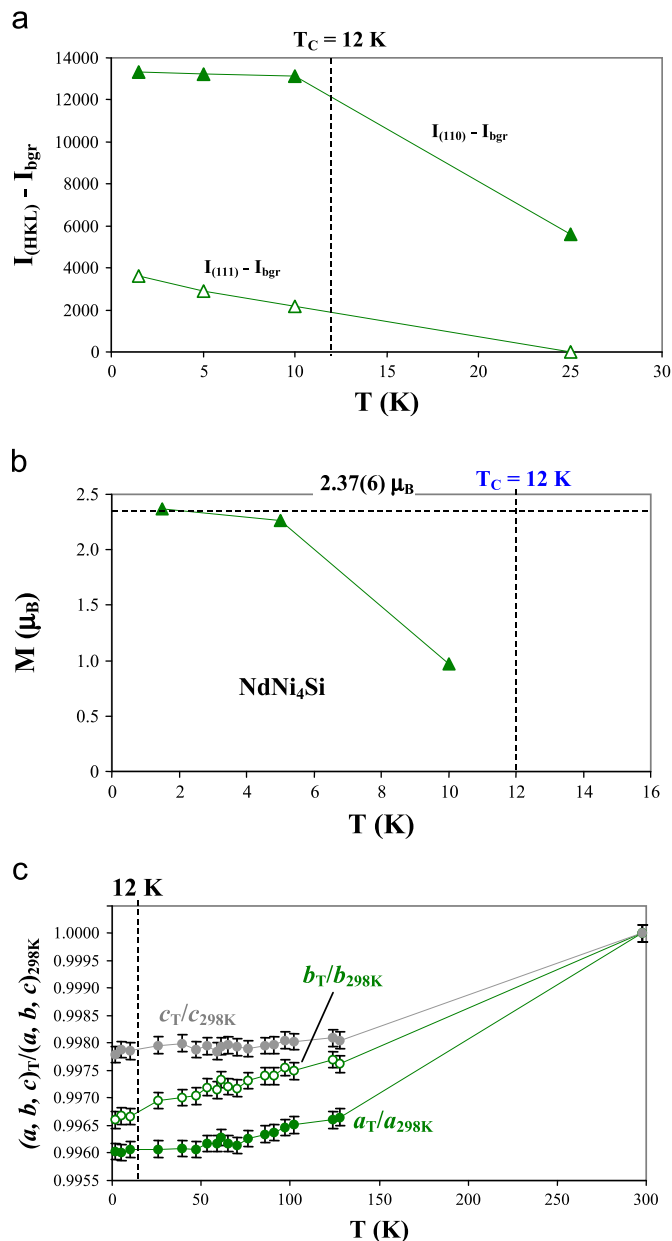
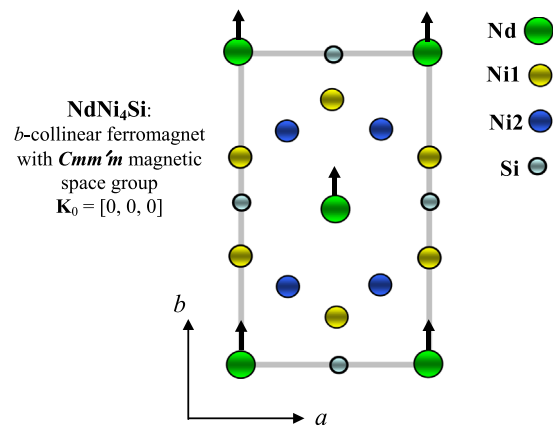


Fig. 3. Neutron diffraction patterns of  $\text{NdNi}_4\text{Si}$  (a) at 25 K (paramagnetic state) and (b) at 1.5 K ( $b$ -axis ferromagnet with  $\mathbf{K}_0=[0, 0, 0]$  wave vector). The first row of ticks refers to the nuclear Bragg peaks whereas the second row of lines refers to the magnetic reflections. The  $(hkl)$  of strongest magnetic reflections are indicated in (b).



**Fig. 4.** Thermal evolution of (a) strongest magnetic reflections  $I_{(hkl)}$  in the neutron diffraction patterns of NdNi<sub>4</sub>Si, (b) the magnetic moments of Nd atom (along the  $b$  axis) and (c) of relative cell parameters  $a_T/a_{298K}$ ,  $b_T/b_{298K}$  and  $c_T/c_{298K}$ . Here  $a_T$ ,  $b_T$ ,  $c_T$ ,  $a_{298K}$ ,  $b_{298K}$  and  $c_{298K}$  are cell parameters of NdNi<sub>4</sub>Si at a given temperature  $T$  and 298 K, respectively.

A commensurate  $b$ -axis collinear ferromagnetic model of NdNi<sub>4</sub>Si fits best with the NDP data (Fig. 5). Within this model, the calculated magnetic moments for the Ni1 and Ni2 sublattices are close to or within the error bar with  $M_{Ni} \sim 0.13(15) \mu_B$ , which means that the significance of such ordered magnetic moment on Ni cannot be confirmed. The other tested commensurate variants yielded no magnetic ordering for the Ni sublattices either. The negligible presence of the Ni magnetic moments in this compound results most probably from the Ni-3d band filling via electronic hybridization with the Nd and Ni neighbor states. The  $b$ -collinear magnetic ordering of the Nd sublattice corresponds to the  $Cmm'm$  magnetic space group as shown in Table 1. The neodymium magnetic moment reaches  $2.37(5) \mu_B$  at 1.5 K, a value less than the theoretical value of  $3.27 \mu_B$  expected for Nd magnetic moment [26] (Fig. 4b and Table 2), which is often observed in some rare-earth-based intermetallic compounds [27,28].



**Fig. 5.** The magnetic structure of YNi<sub>4</sub>Si-type NdNi<sub>4</sub>Si with  $b$ -axis collinear ferromagnetic ordering of Nd sublattice below  $\sim 12$  K of  $Cmm'm$  magnetic space group ( $\mathbf{K}_0 = [0, 0, 0]$  wave vector).

The unit cell of NdNi<sub>4</sub>Si undergoes anisotropic distortion down to the ferromagnetic transition temperature: the cell parameters decrease with  $a_T/a_{298K} < b_T/b_{298K} < c_T/c_{298K}$ , and below the ferromagnetic ordering the cell parameters remain almost constant (Fig. 4c and Table 2). As the NdNi<sub>4</sub>Si structure is an orthorhombically distorted variant of the hexagonal CaCu<sub>5</sub> structure, the  $b/3^{1/2}a$  ratio can be used to estimate the degree of the distortion and its progression with temperature. The  $b/3^{1/2}a$  ratio stays almost constant from 298 K to 1.5 K and it is far from the unit value that corresponds to the transformation from the orthorhombic YNi<sub>4</sub>Si-type lattice to the hexagonal CaCu<sub>5</sub>-type lattice.

## 5. Discussion

The saturation magnetization at 2 K and in 50 kOe yielded a magnetic moment of  $1.1 \mu_B$  per neodymium atom (Fig. 1b), whereas neutron diffraction studies at 1.5 K and in a zero applied field indicated a complete ferromagnetic ordering of NdNi<sub>4</sub>Si with  $2.37 \mu_B/\text{Nd}$  (Fig. 4b). It can be understood that a large magnetic anisotropy prevents a parallel alignment of all the Nd moments in the polycrystalline sample with the magnetic field even at 50 kOe.

Falkowski et al. [16] reported the magnetic properties of CaCu<sub>5</sub>-type NdNi<sub>4</sub>Si compound unfortunately without providing crystal data. Based on the aforementioned structural and magnetic data, we propose that transformation from the initial CaCu<sub>5</sub>- to the YNi<sub>4</sub>Si-type NdNi<sub>4</sub>Si unit cell (compression along the  $b$ -orthorhombic axis as in TbNi<sub>4</sub>Si [12]) leads to the modification in the Nd environment and thus the changes in their magnetic properties, such as, increasing of temperature of magnetic ordering from 9.2 K up to 12 K, reorientation of the neodymium moments in the  $ab$ -plane normal to the compression of unit cell, decreasing of magnetocaloric effect from  $-7.3 \text{ J/kg K}$  of CaCu<sub>5</sub>-type NdNi<sub>4</sub>Si down to  $-3.3 \text{ J/kg K}$  of YNi<sub>4</sub>Si-type NdNi<sub>4</sub>Si in field of 0–50 kOe as in TbNi<sub>4</sub>Si [12]. Such a transformation leads to the appearance of distinct hysteresis loop at 2 K of the YNi<sub>4</sub>Si-type NdNi<sub>4</sub>Si in contrast with the CaCu<sub>5</sub>-type NdNi<sub>4</sub>Si (Table 3).

## 6. Conclusions

The new YNi<sub>4</sub>Si-type NdNi<sub>4</sub>Si supplements the series of YNi<sub>4</sub>Si-type RNi<sub>4</sub>Si compounds with  $R = \text{Y, La, Ce, Sm, Gd-Ho}$ . Compared to the CaCu<sub>5</sub>-type NdNi<sub>4</sub>Si compound, the YNi<sub>4</sub>Si-type counterpart has the relatively high ferromagnetic ordering temperature (9.2 K vs. 12 K), the small magnetocaloric effect ( $-7.3 \text{ J/kg K}$  vs.  $-3.3 \text{ J/kg K}$  for  $\Delta H = 50 \text{ kOe}$ ), and the large magnetic anisotropy at low

**Table 2**

Crystallographic and magnetic parameters of YNi<sub>4</sub>Si-type NdNi<sub>4</sub>Si at different temperatures: cell parameters *a*, *b* and *c*, unit cell volume *V*, *b*/(3<sup>1/2</sup>*a*) ratio, the atomic position of Ni1 atom *y*<sub>Ni1</sub><sup>a</sup>, *M*<sub>B</sub><sup>K<sub>0</sub></sup> the magnetic moments of Nd along the *b*-axis with **K**<sub>0</sub>=[0, 0, 0] wave vector. Reliability factors are: *R*<sub>F</sub> for the crystal structure and *R*<sub>P</sub><sup>b</sup> for the magnetic structure.

T (K)	Cell parameters (nm)	<i>V</i> (nm <sup>3</sup> )	<i>b</i> /(3 <sup>1/2</sup> <i>a</i> )	<i>y</i> <sub>Ni1</sub>	<i>R</i> <sub>F</sub> (%)	Atom	<i>M</i> <sub>B</sub> <sup>K<sub>0</sub></sup> (μ <sub>B</sub> )	<i>R</i> <sub>P</sub> <sup>b</sup> (%)
298 <sup>b</sup>	<i>a</i> =0.51354(2) <i>b</i> =0.83006(3) <i>c</i> =0.39707(1)	0.16926(4)	0.93320(5)	0.3424(5)	4.5			
128	<i>a</i> =0.51259(5) <i>b</i> =0.82933(9) <i>c</i> =0.39689(4)	0.16872(9)	0.93411(9)	0.3411(3)	3.6			
25	<i>a</i> =0.51224(5) <i>b</i> =0.82865(9) <i>c</i> =0.39678(3)	0.16842(9)	0.93398(9)	0.3412(3)	3.4			
10	<i>a</i> =0.51229(4) <i>b</i> =0.82854(7) <i>c</i> =0.39682(3)	0.16843(9)	0.93376(8)	0.3413(3)	3.6	Nd <sup>1</sup> , Nd <sup>2</sup>	0.97(12)	9.1
5	<i>a</i> =0.51226(4) <i>b</i> =0.82855(7) <i>c</i> =0.39683(3)	0.16843(8)	0.93383(8)	0.3410(2)	3.1	Nd <sup>1</sup> , Nd <sup>2</sup>	2.26(6)	5.4
1.5	<i>a</i> =0.51228(4) <i>b</i> =0.82849(6) <i>c</i> =0.39679(2)	0.16841(7)	0.93373(7)	0.3412(2)	3.0	Nd <sup>1</sup> , Nd <sup>2</sup>	2.37(5)	5.4

<sup>a</sup> Atomic sites of YNi<sub>4</sub>Si-type NdNi<sub>4</sub>Si (space group *Cmmm*): Nd (2*a*) [0, 0, 0], Ni1 (4*i*) [0, 0.3424(5), 0], Ni2 (4*f*) [1/4, 1/4, 1/2] and Si (2*c*) [0, 1/2, 1/2].

<sup>b</sup> X-ray data.

**Table 3**

Magnetic properties of CaCu<sub>5</sub>-type NdNi<sub>5</sub>, NdNi<sub>4</sub>Si and YNi<sub>4</sub>Si-type NdNi<sub>4</sub>Si compounds.

Compound	Type structure	$\theta_P$ (K)	<i>M</i> <sub>eff</sub> (μ <sub>B</sub> /fu)	<i>T</i> <sub>C</sub> (K)	<i>M</i> <sub>sat</sub> (μ <sub>B</sub> /fu)	<i>M</i> <sub>res</sub> (μ <sub>B</sub> /fu) (2 K)	<i>H</i> <sub>coer</sub> (kOe)(2 K)	$\Delta S_m$ (J/kg K) (0–50 kOe)	Ref.
NdNi <sub>5</sub>	CaCu <sub>5</sub>			7.2	2.1			–8.45	[14,15]
NdNi <sub>4</sub> Si	CaCu <sub>5</sub>			9.2	1.5 (4.2 K, 90 kOe)	–	–	–7.3	[16]
NdNi <sub>4</sub> Si	YNi <sub>4</sub> Si	–21	3.8	12	1.1 (2 K, 50 kOe)	0.8	–3.0	–3.3	<sup>a</sup>

<sup>a</sup> This work.

temperatures. This work suggests that such an orthorhombic distortion from the initial CaCu<sub>5</sub>-type unit cell can take place in the other YNi<sub>4</sub>Si-type solid solutions, e.g., PrNi<sub>4</sub>Si. The orthorhombic distortion may be used as a prospective route for optimization of permanent magnetic properties in the family of CaCu<sub>5</sub>-type rare earth materials.

## Acknowledgments

This work was supported by the Russian Fund for Basic Research (Grant nos. 12-03-00428-a and 13-02-00916), the National Natural Science Foundation of China (Grant no. 51301116), and the Natural Science Foundation of Jiangsu Province (Grant no. BK20130261). The Institute Laue Langevin (Grenoble, France) is warmly acknowledged for the use of the neutron diffraction beam. Y.S.K. thank “Regional Materials Science and Technology Centre – Feasibility Program” of Czech Republic under Grant nos. CZ.1.07/2.3.00/30.0016 and LO1203 for financial support.

## References

- [1] A.V. Morozkin, A.V. Knotko, V.O. Yapaskurt, Fang Yuan, Y. Mozharivskiy, R. Nirmala, J. Solid State Chem. 208 (2013) 9–13.
- [2] P. Villars, L.D. Calvert, Pearson's Handbook of Crystallographic Data for Intermetallic Phases, ASM International, Materials Park, Ohio, 1985.
- [3] SpringerMaterials The Landolt-Börnstein Database – Materials Science Data for 250000 Substances < http://www.springermaterials.com > .
- [4] K.J. Strnat, Ferromagnetic materials, in: E.P. Wohlfarth, K.H.J. Buschow (Eds.), Elsevier Science, 131th ed., North-Holland, Amsterdam, 1988.
- [5] E. Burzo, A. Chelkowski, H.R. Kirchmayr, Magnetic Properties of Metals, 248th ed., Springer-Verlag, Landolt-Burnstein, 1990.
- [6] S.N. Klyamkin, V.N. Verbetsky, A.A. Karih, J. Alloy. Compd. 231 (1995) 479–482.
- [7] T. Tolinski, M. Falkowski, K. Synoradzki, A. Hoser, N. Stuber, J. Alloy. Compd. 523 (2012) 43–48.
- [8] N. Bucur, E. Burzo, R. Tetean, J. Optoelectron. Adv. Mater. 10 (2008) 801.
- [9] M. Falkowski, B. Andrzejewski, A. Kowalczyk, J. Alloy. Compd. 442 (2007) 155–157.
- [10] L. Morellon, P.A. Algarabel, M.R. Ibarra, A.D. Moral, D. Gignoux, D. Schmitt, J. Magn. Magn. Mater. 153 (1996) 17.
- [11] G. Aubert, D. Gignoux, B. Hennion, B. Michelutti, A.N. Saada, Solid State Commun. 37 (1981) 741–743.
- [12] A.V. Morozkin, F. Yuan, Y. Mozharivskiy, O. Isnard, J. Magn. Magn. Mater. 368 (2014) 121–125.
- [13] A.V. Morozkin, R. Nirmala, S.K. Malik, J. Magn. Magn. Mater. 378 (2015) 221–227.
- [14] R.J. Radwanski, N.H.K. Ngan, J. Alloy. Compd. 219 (1995) 260–263.
- [15] P.J. von Ranke, M.A. Mota, D.F. Grangeia, A.M.G. Carvalho, F.C.G. Gandra, A.A. Coelho, A. Caldas, N.A. de Oliveira, S. Gama, Phys. Rev. B 70 (2004) 134428.
- [16] M. Falkowski, T. Tolinski, A. Kowalczyk, Acta Phys. Pol. A 121 (2012) 1290–1292.
- [17] < www.ill.eu > , Yellow Book.
- [18] F. Izumi, in: R.A. Young (Ed.), The Rietveld Method, Oxford University Press, Oxford, 1993, p. 13.
- [19] F. Izumi, Rigaku J., vol. 6, 1989, pp. 10.
- [20] R.A. Levy, Principles of Solid State Physics, Academic Press, New York, 1968.
- [21] A.M. Tishin, Y.L. Spichkin, The Magnetocaloric Effect and its Applications, Institute of Physics Publishing, Bristol, Philadelphia (2003) 480.
- [22] J. Rodriguez-Carvajal, Physica B 192 (1993) 55–69.

- [23] C.J. Bradley, A.P. Cracknell, *The Mathematical Theory of Symmetry in Solids*, Clarendon, Oxford, 1972.
- [24] D.B. Litvin, *Magnetic Group Tables, 1-, 2- and 3-Dimensional Magnetic Subperiodic Groups and Magnetic Space Groups*, International Union of Crystallography, Reviewed by the International Union of Crystallography Commission on Magnetic Structures, 2013 ISBN 978-0-9553602-2-0, <http://dx.doi.org/10.1107/9780955360220001>.
- [25] M. Falkowski, M. Pugaczowa-Michalska, A. Kowalczyk, *J. Alloy. Compd.* 577 (2013) 19–24.
- [26] S. Legvold, Rare earth metals and alloys, in: E.P. Wohlfarth (Ed.), *Ferromagnetic Materials*, North-Holland Publishing Company, Amsterdam, 1980, pp. 183–295.
- [27] C. Chacon, O. Isnard, S. Miraglia, *J. Alloy. Compd.* 283 (1999) 320–326.
- [28] C. Zlotea, C. Chacon, O. Isnard, *J. Appl. Phys.* 92 (2002) 7382.